X-Ray Investigations on Annealed Fibers of Poly(*p*-phenylene-1,3,4-oxadiazole)

D. HOFMANN,* R. LEONHARDT, and P. WEIGEL

Institute of Polymer Chemistry, Kantstr. 55, 0-1530 Teltow-Seehof, Germany

SYNOPSIS

The influence of annealing on the supermolecular structure of commercial, thermostable fibers, spun from solutions of poly(*p*-phenylene-1,3,4-oxadiazole) (POD) in H_2SO_4, is examined. The crystalline α-modification of thermally treated POD fibers has an orthorhombic unit-cell probably of space group $P2_12_12_1$. The symmetry of the single POD chain in these crystallites is 2_1. The unit-cell dimensions are $a = 1.235$ nm, $b = 0.655$ nm, $c = 1.40 \cdots 1.47$ nm, where c depends on the annealing temperature T_a. The unit cell contains 4 chains of two monomers each. Annealing up to T_a of about 755 K causes increases in crystallite size, crystalline orientation, and linear degree of order, combined with an improved axial Young's modulus E. Thermal degradation at higher temperatures leads to the breaking of tie molecules in general, while UV-radiation selectively damages tie molecules that are not taut.

INTRODUCTION

Fibers of high thermal stability can be spun from solutions of POD in sulfuric acid.[1-4] The conventional spinning process, resulting in fibers with axial strength at break σ_{br} and Young's modulus E values of < 0.5 GPa and < 20 GPa, respectively, usually consists of three stages: (1) Spinning of the multifilament from a dilute solution (about 1–5 wt %) POD in concentrated (100%) H_2SO_4 in a coagulation bath (usually about a 50 wt % aqueous H_2SO_4 solution); (2) Drawing of the coagulated fiber in the presence of the coagulation agent; (3) Drying of the material and additional drawing at elevated temperatures (up to 570 K). The properties of the spun POD can be further improved by storing it in 75 wt % H_2SO_4 for a few minutes[5] or by annealing.[6,7] It is claimed in some patents[8] that the Inventa AG (Switzerland) has produced POD fibers with σ_{br} up to 2 GPa and E up to 40 GPa by spinning from concentrated solutions of POD in H_2SO_4.

While we have addressed the structure of dilute and concentrated solutions of POD in H_2SO_4 in two previous articles,[9,10] the present investigation mainly is devoted to the influence of thermal annealing on the supermolecular structure of commercial POD fibers. For comparison, the influence of UV-radiation is also considered (Note: POD fibers are highly light-sensitive).

The structure characterization is predominantly based on Wide Angle X-ray Scattering (WAXS) and Small Angle X-ray Scattering (SAXS) investigations. Correlations between supermolecular structure and mechanical properties are qualitatively discussed.

EXPERIMENTAL

Annealing Procedure

A 0.5 m long glass-tube oven, with a diameter of 35 mm, was used for the annealing treatments. The temperature T_a could be kept sufficiently constant ($\pm$ 2 K) in the active annealing region of the oven. The fibers were wound on a 12 cm long stainless steel frame with smooth edges. The ends of the fibers were fixed by knotting. The samples were always brought into the preheated oven. The temperature was measured close to the middle of the respective fiber bundle. Only the material portion that was

* To whom correspondence should be addressed.

Journal of Applied Polymer Science, Vol. 46, 1025–1031 (1992)
 CCC 0021-8995/92/061025-07

above and beneath the sample holder slit during the high temperature treatment was used for further investigations.

Samples

The following samples were investigated:

Sample 1: Commercial POD-multifilament fiber Oksalon (WPV–Chimvolokno, USSR).

Sample 2: As sample 1, but taken from a different lot.

Sample 3: Commercial POD multifilament material (not drawn in the dry state at elevated temperatures).

Sample 4: Obtained from sample 1 via UV-radiation (50 h daylight equivalent).

Sample 5: Obtained from Sample 1 via annealing at fixed ends at T_a = 623 K and t = 30 min.

Sample 6: As sample 5, but T_a = 713 K, t = 5 min.

Sample 7: As sample 6, but T_a = 733 K.

Sample 8: As sample 6, but T_a = 753 K.

Sample 9: As sample 6, but T_a = 768 K.

X-Ray Investigations

Parallelized fiber bundles were utilized as samples in all cases.

A horizontal X-ray counter diffractometer HZG-4A (Freiberger Präzisionsmechanik GmbH, Germany) was used in symmetric transmission mode to scan the meridional and equatorial WAXS. Standard corrections were applied to the data. Crystallite sizes were determined via the Scherrer equation. An azimuthal scan of the main meridional peak at about $2\theta = 25°$ was made for the characterization of the crystalline chain orientation. From this, the half width $\Delta\zeta$ was taken as a rough orientation measure.

In addition, WAXS patterns were obtained for all samples using a vacuum flat film camera in perpendicular transmission (sample-film distance 40 mm) and in transmission with an appropriate inclination of the sample in order to get maximum intensity for the main visible meridional reflection.

The SAXS was registered utilizing a Kissig pinhole, flat-film camera with a sample-film distance of 400 mm. The time of exposure was about 100 h per SAXS pattern.

Mechanical Investigations

Stress–strain curves were recorded at 296 K, using an Instron tensile tester (crosshead speed 10 mm min^{-1}). Young's modulus E and strength at break σ_{br} were obtained from this information.

RESULTS AND DISCUSSION

Figure 1 shows WAXS–fiber patterns for samples 1 and 3. The result for sample 3 (only equatorial and meridional reflections are visible) is characteristic for the so-called β-modification of POD. This term was introduced by Milkova et al.[11] to describe a non-equilibrium solid state phase of POD. This modification is characterized by a quasicrystalline packing of POD chains in two-dimensional layers. Neighboring (x, z)-planes are approximately parallel to each other but do not show any further spatial correlation.

Considering the results of Krasnov et al.[12] on the structure of polyaromatic polymers in general, and data about the conformation of the POD molecule given by Popik et al.[13] and Tsvetkov,[14] the chains in the (x, z)-planes of the β-phase can be characterized as follows (*cf.* also Fig. 2):

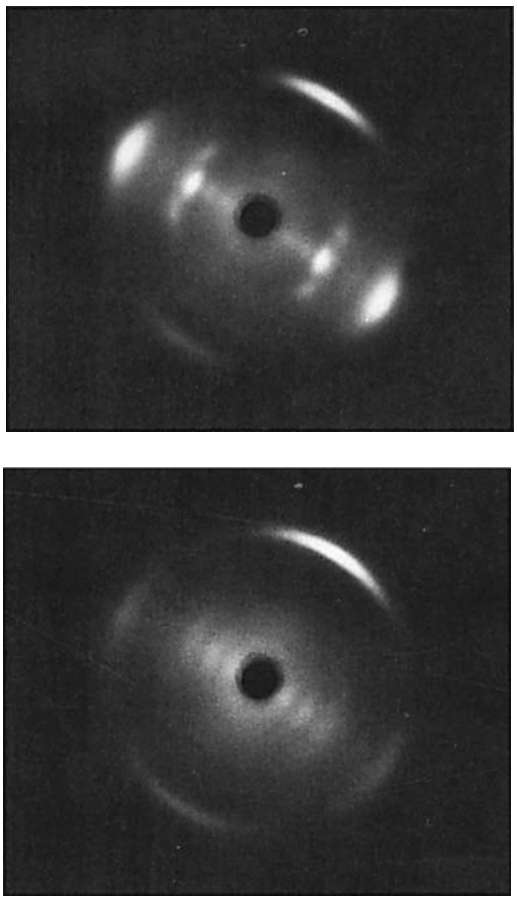

Figure 1 WAXS fiber patterns for samples 1(a) and 3(b) (nonperpendicular transmission/inclination 13°).

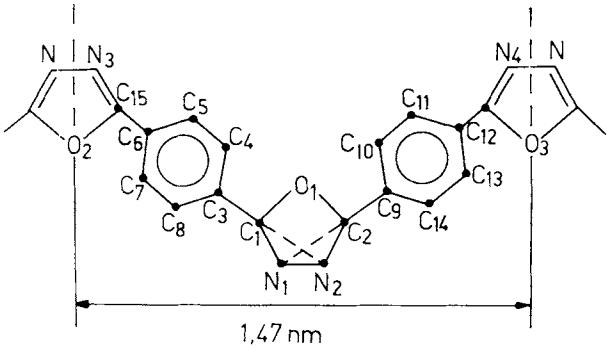

Figure 2 POD conformational repeat unit (*cf.* Ref. 9).

The oxadiazole ring causes a kink of about 40° (angle between C3–C1 and C2–C9 in Fig. 2) in the monomer unit. This feature seems to be crucial for the fact that it is impossible to obtain liquid crystalline solutions of POD in usual solvents.[1] The torsion angles about the two flexible bonds in the monomer C8–C3–C1–N1 and N2–C2–C9–C14 are 45° and −45°, respectively. The plane of the oxadiazole rings is parallel to the (x, z)-plane, while the phenylene rings show an alternating inclination of 45° and −45° relative to the (x, z)-plane. Adjacent chains in the same (x, z)-layer have identical z-coordinates for comparable atoms (Note: In Ref. 11, an angle of 104° is proposed between the x- and the z-axes). The β-modification is usually observed for POD fibers, such as sample 3, that were spun from H_2SO_4 and drawn in the coagulation bath, but were not thermally treated afterwards. Because of the predominant tendency for POD molecules to form two-dimensionally ordered regions in the early stages of the precipitation/drawing process, it is difficult to achieve extended three-dimensional order in the later stages of the sample preparation. One possible way to improve the structure of β-modification POD fibers consists of an additional hot-drawing stage of the dried material, as has happened to samples 1 and 2. The corresponding WAXS data for these samples (*cf.* Fig. 1) are an indication for the α-modification, which shows a certain degree of a distorted three-dimensional order. The main difference in the WAXS–fiber pattern, as compared to the foregoing case, lies in the appearance of off-equatorial reflections. Usual modification α POD-materials often still contain a small amount of the β-phase, as can be concluded from the presence of a WAXS-peak at $2\theta = 10.5°$ that vanishes upon annealing (*cf.* Fig. 3).

Hitherto, a more detailed description of the chain packing in α-modification POD fibers was not given in the literature. The Z-coordinate of the first layer line corresponds to the length of the POD conformational repeat unit, as shown in Figure 2. Thus, the first visible meridional peak at a quarter of this distance can be indexed as (004). This could suggest the presence of a 4-fold screw-axis (4_1 or 4_3) in the unit cell.

The conformational repeat unit, as depicted in Figure 2, contains a 2_1 screw axis along the z-axis (appropriately chosen parallel to the N–N3, N1–N2, and N4–N bonds in the plane of the heterocycles). Therefore, possible tetragonal unit cells could belong to the space groups $P4_12_12$ or $P4_32_12$ with the center chain showing a 90° turnabout and a shift of $c/4$ or $3c/4$ along the crystalline c-axis direction, in comparison to the corner chains. Table I shows the WAXS-peak positions for sample 8 (T_a = 753 K, t = 5 min). The d-values in parentheses are taken from Ref. 11. In comparison to the article by Milkova et al.,[11] we did not get any peak at $2\theta = 8.5°$ (d = 10.4 A). (Note: Metallic sample holders often show a WAXS-peak at about this position, which can cause problems if the WAXS of a sample is registered in symmetric reflection.) However, an additional peak was obtained on the first layer line (d = 0.421 nm).

The smallest tetragonal unit cell that would show a reasonable fit for the peak positions given in Table I (except for the first layer line peak at d = 0.547 nm, where the difference to the calculated d-value is −4%) is $a = b$ = 1.38 nm, c = 1.465 nm. The density for the crystalline phase, however, is much too low in this case (0.3456 g/cm^3 for two chains in the unit cell). Other problems occur with the interpretation of the results of crystallite size measurements (*cf.* Table II) and texture investigations on POD films (to be reported elsewhere[24]) that demand the normals on the lattice planes, giving rise to the two strongest equatorial reflections at a considerable

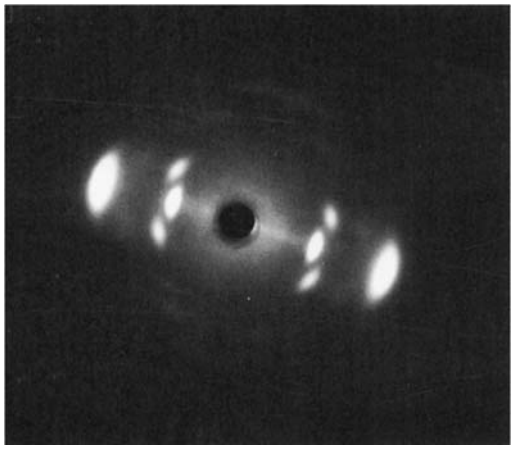

Figure 3 WAXS fiber pattern for sample 8 (perpendicular transmission).

Table I Comparison of Observed and Calculated *d*-Spacings

Layer Line	$2\theta^{obs/o}$	d^{obs}/nm	*hkl*	d^{calc}/nm
0	14.2	0.624	2 0 0	0.618
0	26.9	0.331	0 2 0	0.328
0		(0.166)[a]	0 4 0	0.164
1	16.2	0.547	1 1 1	0.538
1	21.1	0.421	2 1 1	0.430
3	20.0	0.444	1 0 3	0.454
4	24.3	0.366	0 0 4	0.366
6		(0.221)[a]	1 1 6	0.226
7		(0.206)[a]	1 0 7	0.206
8		(0.184)[a]	0 0 8	0.183
10		(0.147)[a]	1 0 10	0.145
11		(0.133)[a]	1 0 11	0.132
12		(0.123)[a]	0 0 12	0.122

[a] Values in parentheses are taken from Ref. 11.

angle towards each other. (Note: These equatorial reflections index as (120) and (140) in the case of the tetragonal unit cell quoted above.)

We have, therefore, considered an orthorhombic unit cell as the next step. The only space groups of this type that show a systematic absence condition $1 \neq 4n$ for (001) peaks are the face centered *Fdd*2 and *Fddd* that are not observed for polymers (cf., e.g., Ref. 25). It is, therefore, necessary to relax the systematic absence condition for meridional reflections to at least $1 \neq 2n$.

A unit cell of $a = 1.235$ nm, $b = 0.655$ nm, $c = 1.465$ nm gives a reasonable fit for all *d*-values (*cf.* Table I). The systematic absence conditions $h \neq 2n$ for (h00). $k \neq 2n$ for (k00), and $1 \neq 2n$ for (001), together with the 2_1 symmetry of the POD conformational repeat unit could indicate a $P2_12_12_1$ symmetry. The density of the crystalline α-POD would be 1.63g/cm^3 (for 4 chains in the unit cell) in this case. This is reasonable, considering the facts that commercial POD fibers of relatively low crystallinity (*cf.* samples 1–3 in Table II) can show density values of about 1.45 g/cm^3, and that the real α-crystallites themselves are probably highly distorted.

Table II Length of the Unit Cell *c* as a Function of the Annealing Temperature T_a

Sample	T_a/K	$2\theta_{004/o}$	*c*/nm
1	—	25.4	1.405
5	623	25.3	1.410
6	713	25.0	1.425
7	733	24.5	1.455
8	753	24.3	1.465
9	768	24.2	1.47

Finally, it should be stressed that there is a slight, but significant, correlation between the length *c* of the unit-cell and the annealing temperature, as will be shown below.

An important qualitative result of the annealing experiments consists in the fact that while sample 5 remained stretched upon annealing (loose after recooling to room temperature) samples 6–9 lost their tautness during the heat treatment. This behavior indicates a usual shrinkage effect for sample 5, but a spontaneous elongation for the latter materials as was already described in the literature.[19]

Table III contains important parameters of the supermolecular structure for the investigated samples. The UV-treatment (*cf.* sample 4) does not result in any significant changes in crystallite sizes, WAXS peak positions, crystalline chain orientation, or linear degree of order. The tensile strength of this material, however, decreased from about 400 MPa before the radiation to about 100 MPa afterwards, while the Young's modulus remained constant. This behavior can be related to light-induced damage in the noncrystalline sample regions. This damage seems to be restricted to chain breaking, for the electron density difference between crystalline and noncrystalline regions is not significantly reduced by the UV-radiation, as indicated by the absence of a visible meridional SAXS reflection.

The annealing of the POD fiber bundles with fixed ends in nitrogen results in an increase of lateral and longitudinal crystallite sizes up to a T_a of about 753 K. This is a typical annealing effect. This growth process stops, however, above a T_a of about 765 K

Table III Quantitative Results of the Supermolecular Structure Investigations

Sample	Average Lateral Crystallite Sizes L_{200}/nm	L_{020}/nm	L_{004}/nm	Meridional Peak Position ($2\theta_{004}$/°)	Half Width of the Azimutal (004)-Scan ($\Delta\zeta$/°)	Meridional SAXS Long Period (L_{SAXS}/nm)	Linear Degree of Order L_{004}/L_{SAXS}
1	4.7	3.0	3.5	25.4	36	Not Visible	(0.33)[a]
2	4.8	2.8	3.8	25.5	33	Not Visible	(0.36)[a]
3	—	(2.2)[b]	(4.1)[b]	(26.2)[b]	38	Not Visible	—
4	4.5	2.8	3.7	25.5	35	Not Visible	(0.35)[a]
5	4.8	2.8	3.6	25.3	37	Not Visible	(0.34)[a]
6	5.1	3.0	3.7	25.0	33	10.5	0.35
7	5.9	3.1	4.2	24.5	31	10.7	0.39
8	6.3	3.6	5.4	24.3	32	10.6	0.51
9	5.7	3.7	5.3	24.2	34	10.6	0.50

[a] Values in parentheses are obtained supposing L_{SAXS} = 10.6 nm.
[b] The *hkl*-indices are not valid for β-POD reflections.

(*cf.* sample 9) obviously due to the beginning of large scale thermal degradation (sample 9 was almost black, while samples 8, 7, and 6 were dark brown, brown, and light brown, respectively).

Another effect of the thermal treatment consists in a systematic decrease of the angular position of the (004) WAXS reflection that remains unchanged after annealing. This effect corresponds to an increased length *c* of the unit cell, as shown in Table II. That is, the unit cell discussed above, utilizing the data in Table I, was just characteristic for sample 8, while the other samples show slightly different *c* and d_{hkl} values. The correlation of *c* with T_a may be related to an increasing kink angle (between C3–C1 and C2–C9 in Fig. 2) of the POD conformational repeat unit. Here it is interesting to note that the length of 1.47 nm for the repeat unit, which was obtained for a kink angle of 46.8°, was reported in Ref. 13 from electron beam diffraction experiments on gaseous 2.5-diphenyl-1,3,4-oxadiazole (DOD) at elevated temperatures. That is, the higher the T_a, the greater the similarity between the geometry of this model compound and the POD conformational repeat unit in modification α crystallites. A less probable cause for the observed d_{004} increase could consist in the transformation of a small percentage of oxadiazole rings in longer hydrazide segments as one result of thermal degradation. In this case, the crystalline lattice would have to be able to accommodate a certain portion of hydrazide units.

The overall level (about 35°) of the crystalline chain axis orientation parameter, $\Delta\zeta$, is considerably higher than that observed for drawn flexible chain materials, such as (high modulus) poly(ethylene) and poly(ethylene terephthalate)-fibers, where $\Delta\zeta$ values of a few degrees (including instrumental broadening) are characteristic.[16,17] POD is a semirigid chain polymer. These materials usually show higher $\Delta\zeta$ parameters in the uniaxially drawn state than flexible chain polymers (*cf.*, for instance, Ref. 18 for the Kevlar example). Thus, the result for POD is not surprising.

The annealing, at a T_a of about 700–755 K, caused a slightly improved axial orientation of the POD chains in the α crystallites, as indicated by $\Delta\zeta$ (*cf.* Table III). This is one contribution to the spontaneous elongation of the POD fibers during annealing at $T_a > 700$ K. Other contributions come from the increase of the linear degree of order L_{004}/L_{SAXS}, which is connected with the increase of the average crystallite length L_{004}. Furthermore, the thermal treatment can result in a partial spontaneous improvement of the axial orientation of chains in the noncrystalline sample regions toward the fiber axis, as was discussed by Kalashnik et al.,[19] and as was confirmed by n.m.r. measurements.[23]

For $T_a > 710$ K (t = 5 min), a meridional SAXS-maximum, related to a meridional long period of 10.6 nm, could be detected. The overall intensity of this scattering increased with increasing T_a. It indicated a serious thermal degradation in the noncrystalline portion of the samples, resulting in an increase of the electron density difference between crystalline and noncrystalline regions. Since the value L_{SAXS} = 10.6 nm did not change significantly for samples 6–9, it was assumed that this held true for the other samples as well (*cf.* Table III). For uniaxially drawn semicrystalline fibers, L_{SAXS} can

be interpreted as the length of the structural unit element composed of a crystallite and one adjacent, noncrystalline region (in fiber axis direction). (Note: Slutsker et al.[20] reported a L_{SAXS} = 15.5 nm for annealed fibers of a 70:30 copolymer of *p*-phenylene-1,3,4-oxadiazole and *m*-phenylene-1,3,4-oxadiazole.)

Table IV contains data on a mechanical investigation for 4 samples. According to Peterlin,[21] the Young's modulus E for uniaxially oriented semicrystalline fibers increased with increasing linear degree of order (crystalline content in the structural unit element) and increasing fraction β of taut tie molecules (*ttm*), connecting two crystallites through a noncrystalline region. In the present case, however, it is inappropriate to make use of the quantitative relations given in Ref. 21 because they become very inaccurate, even for relatively small deviations from a perfectly uniaxial fiber texture (cf. Ref. 22). Therefore, the data given in Table IV will be discussed only qualitatively. Sample 5 was annealed under tension (POD fibers shrink at a temperature of about 620 K). Here, the thermal treatment resulted in a considerably reduced Young's modulus, as compared to the starting material (sample 1). Since the linear degree of order and the orientation factor were about the same for samples 1 and 5, a main effect of the annealing at 623 K was the breaking of a considerable amount of *ttm*. More severe damage to the noncrystalline regions was unlikely because of the still high level of the strength at break for sample 5.

Samples 8 and 9, however, showed spontaneous elongation during the heat treatment. The significant increase of E for sample 8 seemed to be caused mainly by the increase of the linear degree of order (0.33 for sample 1 → 0.51 for sample 8; *cf.* Table III). Although sample 9 revealed about equal crystalline structure parameters as sample 8 (*cf.* Table III), the modulus and strength at break values of the former were only about half as high as for the latter. The thermal degradation that occurred to sample 9 obviously resulted in the breaking of both taut and not taut tie molecules in noncrystalline regions.

Table IV Mechanical Parameters for Selected Samples

Sample	T_a/K	t_a/min	Young's Modulus (E/GPa)	Strength at Break (σ_{br}/MPa)
1	—	—	14.0	395
5	623	30	9.0	420
8	753	5	22.0	350
9	768	5	11.0	190

It is interesting to compare the results for sample 9 with the ones obtained for sample 4 (50 h daylight equivalent UV–radiation), which showed a considerably reduced σ_{br}, but an unchanged E, as compared with sample 1 (starting material), and no meridional SAXS. The UV-radiation probably resulted mainly in the splitting of not taut tie molecules (important for δ_{br}, but not for E), while thermal degradation, besides directly removing material from noncrystalline regions (a lot of gaseous material is set free upon annealing at 768 K and a strong meridional SAXS is observed), splits both taut and not taut tie molecules.

The authors are indebted to Mr. P. Jäckel for the construction of the annealing oven.

REFERENCES

1. A. H. Frazer and F. T. Wallenberger, *J. Polym. Sci.*, **A2,** 1171 (1964).
2. Y. Iwakura, K. Uno, and S. Hara, *J. Polym. Sci.*, **A3,** 45 (1965).
3. A. T. Kalashnik, A. V. Volokhina, A. S. Semenova, L. K. Kusnezova, and S. P. Papkov, *Chim.*, **1,** 46 (1978).
4. N. I. Bobrovnickaja, V. V. Romanov, A. T. Kalashnik, W. E. Sorokin, A. S. Semenova, and R. A. Makarova, *Chim.*, **1,** 42 (1983).
5. V. S. Matwejew, *Chim.*, **3,** 17 (1984).
6. J. Preston, W. B. Black, and W. L. Hofferbert, *J. Macromol. Sci.*, **A7,** 45 (1973).
7. J. Preston, W. B. Black, and J. W. Morgan, *J. Macromol. Sci.*, **A7,** 325 (1973).
8. Inventa AG (Switzerland): US-PS 3 992 504 (1979), GB-PS 1468 934 (1977).
9. D. Hofmann, P. Weigel, J. Ganster, and H.-P. Fink, *Polymer,* **32,** 284 (1991).
10. H. Schelle, D. Hofmann, and P. Weigel, *Acta Polym.*, **40,** 450 (1989).
11. L. P. Milkova, V. V. Romanov, N. C. Pozhalkin, N. P. Krutchynin, W. G. Kulichygin, and M. B. Schablygin, *Chim.*, **3,** 323 (1986).
12. E. P. Krasnov, A. E. Stepanyan, Yu. I. Mitchenko, Yu. A. Tolkachev, and N. W. Lukacheva, *Vysokomol. Soed.*, **A19,** 1566 (1977).
13. N. I. Popik, M. V. Shablygin, L. V. Vilkov, A. S. Semenova, and T. V. Kradchenko, *Vysokomol. Soed.*, **B25,** 38 (1983).

14. V. N. Tsvetkov, *Vysokomol. Soed.*, **A19,** 2171 (1977).
15. D. L. Brydon, I. S. Fisher, J. Emans, D. M. Smith, and W. A. MacDonald, *Polymer,* **30,** 619 (1989).
16. E. Schulz, A. Bauer, and D. Hofmann, *Acta Polym.* **39,** 181 (1988).
17. D. Hofmann, U. Göschel, E. Walenta, D. Geiß, and B. Philipp, *Polymer,* **30,** 242 (1989).
18. A. M. Hindeleh, N. A. Halim, and K. A. Ziq, *J. Macromol. Sci. Phys.*, **B23,** 289 (1984).
19. A. T. Kalashnik, A. V. Volokhina, A. S. Semenova, L. K. Kusnezova, and S. P. Papkov, *Chim.*, **4,** 51 (1977).
20. L. I. Slutzker, Z. Yu. Chereiskin, L. E. Utevski, V. N. Kuz'min, A. S. Semonova, and A. V. Volokhina, *Vysokomol. Soed.*, **A17,** 2080 (1975).
21. A. Peterlin, in *Ultra High Modulus Polymers,* A. Ciferri and I. M. Ward, Eds., Applied Science, London, 1979.
22. C. W. M. Bastiaansen, P. J. R. Leblans, and P. Smith, *Macromolecules,* **23,** 2365 (1990).
23. A. N. Grebenkin, I. A. Gorshkova, A. I. Kol'tsov, N. P. Okromchedlidze, R. A. Makarova, A. V. Savitskii, and G. N. Shmikk, *Vysokomol. Soed.*, **29B,** 64 (1987).
24. B. Schulz, R. Schmolke, D. Hofmann, and E. Leibnitz, submitted for publication in *Makromol. Chem.*
25. B. Wunderlich, *Macromolecular Physics,* Vol. 1, Academic, New York, London, 1973.

Received September 23, 1991
Accepted January 2, 1992